Fast revascularization of the injured area is essential to support zebrafish heart regeneration

Rubén Marín-Juez[a,1], Michele Marass[a], Sebastien Gauvrit[a], Andrea Rossi[a], Shih-Lei Lai[a], Stefan C. Materna[b], Brian L. Black[b,c], and Didier Y. R. Stainier[a,1]

[a]Department of Developmental Genetics, Max Planck Institute for Heart and Lung Research, 61231 Bad Nauheim, Germany; [b]Cardiovascular Research Institute, University of California, San Francisco, CA 94143-3120; and [c]Department of Biochemistry and Biophysics, University of California, San Francisco, CA 94143

Edited by Margaret Buckingham, Pasteur Institute, Paris, France, and approved August 9, 2016 (received for review April 4, 2016)

Zebrafish have a remarkable capacity to regenerate their heart. Efficient replenishment of lost tissues requires the activation of different cell types including the epicardium and endocardium. A complex set of processes is subsequently needed to support cardiomyocyte repopulation. Previous studies have identified important determinants of heart regeneration; however, to date, how revascularization of the damaged area happens remains unknown. Here, we show that angiogenic sprouting into the injured area starts as early as 15 h after injury. To analyze the role of *vegfaa* in heart regeneration, we used *vegfaa* mutants rescued to adulthood by *vegfaa* mRNA injections at the one-cell stage. Surprisingly, *vegfaa* mutants develop coronaries and revascularize after injury. As a possible explanation for these observations, we find that *vegfaa* mutant hearts up-regulate the expression of potentially compensating genes. Therefore, to overcome the lack of a revascularization phenotype in *vegfaa* mutants, we generated fish expressing inducible dominant negative Vegfaa. These fish displayed minimal revascularization of the damaged area. In the absence of fast angiogenic revascularization, cardiomyocyte proliferation did not occur, and the heart failed to regenerate, retaining a fibrotic scar. Hence, our data show that a fast endothelial invasion allows efficient revascularization of the injured area, which is necessary to support replenishment of new tissue and achieve efficient heart regeneration. These findings revisit the model where neovascularization is considered to happen concomitant with the formation of new muscle. Our work also paves the way for future studies designed to understand the molecular mechanisms that regulate fast revascularization.

heart regeneration | angiogenesis | revascularization | coronaries | VEGF

Cardiomyopathies are a leading cause of morbidity and mortality in developed countries, where one in five people is predicted to develop heart failure. Moreover, hospitalizations caused by these cardiomyopathies have increased in the last decade by more than 20% (1). After injury, damaged tissue is replaced by a fibrotic scar instead of new muscle, and this scarring compromises contractility and permanently alters tissue architecture. These changes lead to pathological tissue remodeling and heart failure. Recent findings indicate that, contrary to long-standing dogma, the mammalian heart retains cardiomyocyte (CM) self-renewal capacity (2, 3). Therefore, understanding mechanisms underlying cardiac regeneration is key to developing therapies to boost the endogenous regenerative machinery of the heart.

Unlike the mammalian heart, the zebrafish heart is able to regenerate following different types of severe insults (4–8). In zebrafish, the main source of the newly formed CMs is reported to arise by proliferation of preexisting CMs following their dedifferentiation (9, 10). Other tissues such as the epicardium and endocardium are activated upon injury. Similar to the myocardium, following-injury epicardial cells exhibit morphological changes and reexpress developmental genes including *raldh2 and tbx18* (11, 12). The epicardium gives rise to myofibroblasts and perivascular cells (13, 14), and epicardium-derived perivascular and smooth muscle cells support revascularization of the injured area in zebrafish and mammals (15, 16). Following injury, new coronary vessels penetrate the damaged area (5, 12, 16) where the main source of new coronary endothelium is preexisting endothelium (17). Fgf and Pdgf signaling have been reported to be important for neovascularization during heart regeneration (12, 16). Interference with Fgf signaling by overexpression of dominant negative Fgfr1 prevents heart regeneration by diminishing epicardial invasion of the wound, neovascularization, and myocardial regeneration (12). Similarly, pharmacological inhibition of Pdgf signaling reduces epicardial proliferation and neovascularization (16). However, how neovascularization takes place in a vertebrate model with cardiac regenerative capacity remains unknown. Here, using different zebrafish endothelial specific reporter lines, we have observed coronary vessels sprouting into the injured area as early as 15 h after injury (hpi), and a coronary plexus within 2 d after injury (dpi).

VEGFA is a key regulator of vasculogenesis and angiogenesis (18). In pathological hypertrophy and advanced stages of heart failure, VEGFA levels are depleted and the number of vascular beds reduced dramatically (19), limiting the capacity of the heart to generate new vessels. *Vegfa* knockout mice die before birth (18). However, mice that lack only two of the main VEGFA isoforms ($VEGF_{164}$ and $VEGF_{188}$) survive to adulthood but die of ischemic cardiomyopathy and display fewer and irregular coronaries (20). Conversely, a recent study by Zangi et al. showed that rapid post-infarction administration of human VEGFA by modified RNA injection stimulated neovascularization and improved myocardial performance and survival after myocardial infarction in mice (21). To understand which factors allow the zebrafish heart to achieve fast and efficient revascularization, we rescued and grew to adulthood

Significance

A heart attack occurs when blood flow to part of the heart is blocked, and oxygen and nutrients are unable to reach that tissue, irreversibly damaging cardiac muscle cells. Dead muscle cells are replaced by a noncontractile scar that affects cardiac function. Unlike humans, zebrafish can regenerate their heart after injury, replacing the scarred tissue with new cardiomyocytes. Understanding the mechanisms zebrafish deploy to regenerate their heart may help us design more efficient therapies for human heart disease. In this study, we show that to regenerate their heart, zebrafish quickly revascularize the damaged area, and that this ability to revascularize is temporally restricted.

Author contributions: R.M.-J. and D.Y.R.S. designed research; R.M.-J., M.M., S.G., S.-L.L., and S.C.M. performed research; R.M.-J., M.M., A.R., S.C.M., and B.L.B. contributed new reagents/analytic tools; R.M.-J., M.M., S.G., S.-L.L., and D.Y.R.S. analyzed data; and R.M.-J., S.C.M., B.L.B., and D.Y.R.S. wrote the paper.

The authors declare no conflict of interest.

This article is a PNAS Direct Submission.

Data deposition: The data reported in this paper have been deposited in the Gene Expression Omnibus (GEO) database, www.ncbi.nlm.nih.gov/geo (accession no. GSE78945).

[1]To whom correspondence may be addressed. Email: ruben.marin-juez@mpi-bn.mpg.de or didier.stainier@mpi-bn.mpg.de.

This article contains supporting information online at www.pnas.org/lookup/suppl/doi:10.1073/pnas.1605431113/-/DCSupplemental.

CELL BIOLOGY

zebrafish homozygous *vegfaa* mutants by injecting *vegfaa* mRNA at the one-cell stage. Surprisingly, *vegfaa*$^{-/-}$ adult fish developed a coronary network and were able to revascularize the injured area, allowing cardiac regeneration.

To gain insight into the role of fast angiogenic revascularization during heart regeneration, we engineered an inducible transgenic line expressing a dominant negative Vegfaa isoform (dn-Vegfaa). Using this tool, we were able to efficiently block coronary sprouting after injury. Importantly, our results also show that the ability to revascularize the damaged area is temporally restricted, and blockade of fast coronary invasion prevents tissue replenishment leading to the formation of a fibrotic scar. These results suggest that acceleration of vascular invasion of the injured area may be an attractive therapeutic strategy to achieve efficient heart regeneration.

Results

Coronary Vessels Invade the Damaged Area Early After Injury. The zebrafish heart can regenerate after resection, genetic ablation of CMs, and cryoinjury (4–8). Cryoinjury closely models myocardial infarction because the damaged region is retained after injury, being replaced by a scar that will later be substituted by healthy tissue (5–7). The persistence of the damaged tissue also allows visualization of the revascularization process.

We cryoinjured adult hearts expressing the endothelial-specific transgene *fli1a:EGFP* (Fig. 1*A*) and found that at 15 hpi, coinciding with endothelial proliferation in the ventricular wall (Fig. S1*A*), the first vessel sprouts were entering the injured zone (Fig. 1*B*). By 40 hpi, a vascular plexus had formed in close proximity to the border zone, and large vessels were observed invading the damaged region, moving toward the apex (Fig. 1*C*). Revascularization started mainly from vessels coming from the dorsal half of the ventricle [i.e., vessels located on the surface of the ventricle that faces the atrium, close to the atrioventricular canal (AVC); Fig. S1 *B–C″*]. Based on their location on the surface of the heart, we postulate that the vascular sprouts entering the injured zone are coming from preexisting coronary vessels (Fig. S1*B*). It has been shown that epicardial cells are activated early after cryoinjury and partially repopulate the damaged area by 3 dpi (5, 6). To investigate whether any epicardial cells could be observed in the injured area by 15 hpi, we cryoinjured fish harboring the *tcf21:DsRed2* transgene, which labels epicardial and epicardium-derived cells (EPDCs) (14). However, at 15 hpi, we did not observe any DsRed^{+} cells in the damaged region, indicating that blood vessels enter the injury site before EPDCs (Fig. S2).

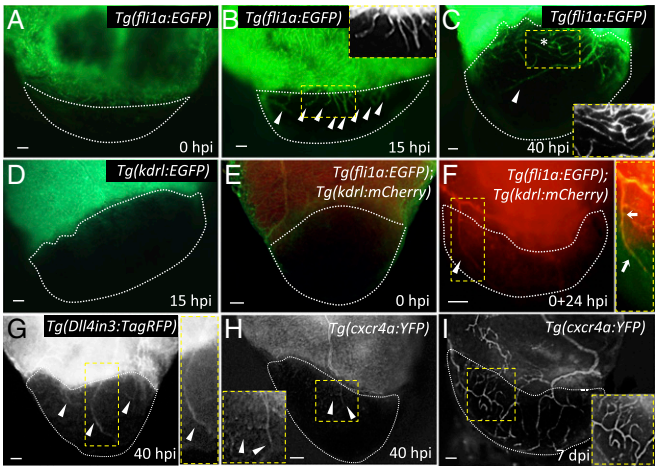

Fig. 1. The zebrafish heart displays fast revascularization of the damaged area. (*A–C*) *Tg(fli1a:EGFP)* ventricles at 0, 15, and 40 hpi. White arrowheads point to coronary vessel sprouts in the injured area; asterisk marks an area of coronary plexus (n = 4). *Insets* show high-magnification images of early coronary sprouts (*B*) and the coronary plexus (*C*). (*D*) *Tg(kdrl:EGFP)* heart at 15 hpi (n = 3). (*E* and *F*) *Tg(fli1a:EGFP);Tg(kdrl:mCherry)* ventricles extracted at 0 hpi and cultured in explant medium for 24 h (0+24 hpi) (n = 3). White arrowhead points to *kdrl*:EGFP^{+} vessels sprouting into the injured area. *Inset* shows overlay image of a sprouting coronary vessel. White arrows point to *fli1a*:EGFP^{+}/*kdrl*:mCherry^{+} coronary vessel sprouting into the injured area. (*G*) *Tg(Dll4in3:TagRFP)* ventricle at 40 hpi (n = 5). *Inset* shows a *Dll4in3*:TagRFP^{+} sprouting coronary artery. (*H* and *I*) *Tg(cxcr4a:YFP)* ventricles at 40 hpi (n = 3) and 7 dpi (n = 4). *Insets* show *cxcr4a*:YFP^{+} sprouting coronaries; white arrowheads point to coronary arteries sprouting into the injured area. Dotted lines delineate the injured area. (Scale bars: 50 μm.)

To assess when the first invading vessels express arterial markers, cryoinjury was performed in *Tg(kdrl:EGFP)* and *Tg(-0.8flt1:RFP)* lines, reported to show fluorescent protein expression mainly in arteries at early developmental stages (22, 23). We first used the caudal fin to test whether these transgenes label arteries in adult animals. The caudal fin is composed of several fin rays each perfused by a single medial artery and two lateral veins (24). We observed that although *Tg(kdrl:*EGFP) expression was restricted to the medial artery in the fin (Fig. S3*A*), *Tg(-0.8flt1:*RFP*)* expression was observed in nearly all vessels in the fin (Fig. S3*B*) and heart (Fig. S1 *B* and *C*). In view of these results, we chose *Tg(kdrl:EGFP)* as an arterial marker in adult fish.

Following injury, we did not find any *kdrl:*EGFP^{+} vessels invading the injury site at 15 hpi, indicating that early vascular sprouts are not arterial (Fig. 1*D*). To assess when the first arteries appear in the damaged region, we used a previously described heart explant model (25). In that system, hearts explanted immediately after injury displayed *kdrl:*mCherry^{+} vessels in the injury site after 24 h in culture (Fig. 1 *E* and *F*). Moreover, we noticed that the first vessels to invade the injured area were initially *fli1a:* EGFP^{+}, but by 24 hpi, some vessels began to express the *kdrl:* mCherry arterial marker (Fig. 1*F*). These observations support the notion that, as shown in the caudal fin regeneration model (24), once the vascular plexus is formed, some vessels gain arterial identity. To further test whether arterial specification is a late event during revascularization, we developed an arterial-specific reporter line by using a previously described enhancer of the mouse *Dll4* gene (26), *Tg(Dll4in3:TagRFP)*. This line expresses TagRFP specifically in arterial endothelium in both embryos (Fig. S3 *C–E*) and adults (Fig. S3*F*). Using this line, we confirmed our observations that the first vessels to invade the damaged area initially do not express arterial markers (Fig. S3*G*) and found that *Dll4in3:* TagRFP expression was evident by 40 hpi (Fig. 1*G*). To investigate whether some invading vessels also express venous markers, we cryoinjured the hearts of *Tg(flt4:YFP)* fish. As shown, coronary vessels down-regulating arterial markers did not display *flt4:*YFP expression (27); indeed, we observed only a few *flt4:*YFP^{+} vessels, most of which were located in the bulbus arteriosus (Fig. S3*H*).

Lastly, recent studies have shown that during coronary development in zebrafish, migratory vessels express *cxcr4a:YFP*, and upon formation of the coronary network, *cxcr4a:*YFP expression gets restricted to arteries (27). Therefore, to assess whether revascularizing vessels recapitulate the coronary developmental program, we injured *Tg(cxcr4a:YFP)* fish. At 40 hpi, the first *cxcr4a:*YFP^{+} vessels were observed in the injury (Fig. 1*H*), and *cxcr4a:*YFP expression was maintained in vessels in the injured area at 4 and 7 dpi (Fig. S3*I* and Fig. 1*I*). Taken together, these data show that revascularization of the damaged area is a remarkably fast event where, in less than 2 d, a coronary plexus has formed and some vascular sprouts invading the injured zone have activated the expression of arterial markers.

***vegfaa* Mutant Hearts Develop Coronary Vessels and Regenerate.** To gain insight into the mechanisms underlying fast revascularization, we examined the expression of *vegfaa* and *vegfab*, the zebrafish orthologs of *Vegfa*, by quantitative PCR (qPCR) (primer sequences

in Table S1) at different time points after injury and found that both were expressed (Fig. S4 *A* and *B*); *vegfaa* mRNA levels were significantly elevated early after injury, peaking at 1 dpi and reverting to control levels by 3 dpi (Fig. 2*A*). In contrast, *vegfab* expression levels remained unchanged until 5 dpi (Fig. S4*C*). To further explore the role of *vegfaa* in heart regeneration, we took advantage of a recently generated *vegfaa* mutant (28). *vegfaa*$^{-/-}$ embryos display severe angiogenic defects from an early stage (29). To raise these mutants to adulthood, we rescued them by injecting *vegfaa 121* or *vegfaa 165* mRNA at the one-cell stage. Rescued *vegfaa*$^{-/-}$ embryos develop a functional circulatory loop and survive to adulthood with no overt morphological defects. In rescued *vegfaa* mutant adults, coronaries were distributed irregularly and generally thinner than those in wild-type (WT) fish (Fig. S5 *A* and *B*). Despite this irregular coronary patterning, mutant vessels were luminized and vascular integrity was not compromised (Fig. S5 *C* and *D*), and exhibited *fli1a:*EGFP and *kdrl:*mCherry expression, indicating that arterial specification occurs in *vegfaa*$^{-/-}$ hearts (Fig. S5 *E–E″*). Characterization of cardiac function using echocardiography revealed a significant reduction in heart rate in adult *vegfaa* mutants. This effect was independent of the mRNA used for the rescue or the age of the fish (Fig. S5*F*).

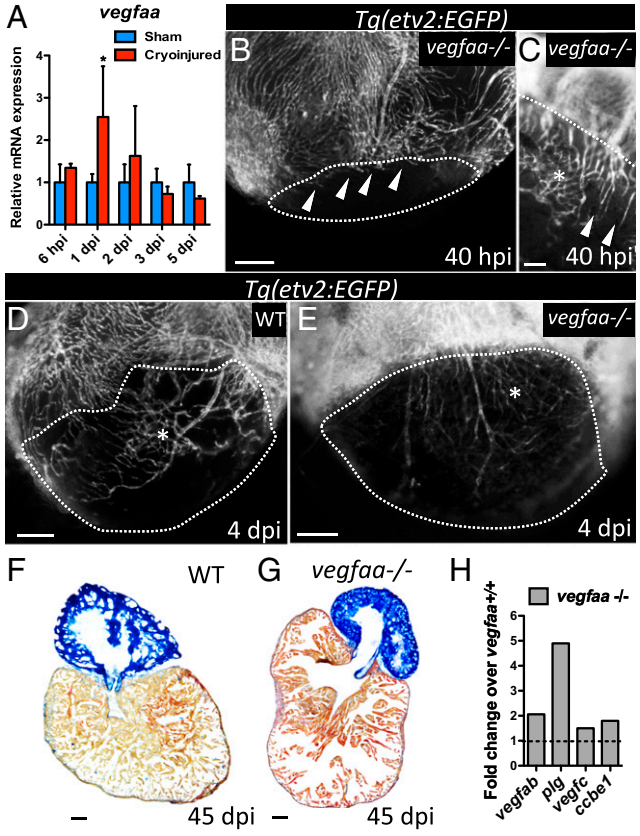

Fig. 2. *vegfaa* mutants exhibit delayed and disorganized revascularization. (*A*) qPCR analysis of *vegfaa* expression at 6 hpi and 1, 2, 3, and 5 dpi. Data are expressed as mean ± SD, **P* < 0.05 (*n* = 4). (*B* and *C*) *Tg(etv2:EGFP) vegfaa*$^{-/-}$ ventricles at 40 hpi (*n* = 3). White arrowheads point to coronary vessels sprouting into the injured area. (*D* and *E*) *Tg(etv2:EGFP)* WT (*n* = 5) and *Tg(etv2:EGFP) vegfaa*$^{-/-}$ ventricles at 4 dpi (*n* = 3). Asterisk marks an area of coronary plexus. Dotted lines delineate the injured area. (*F* and *G*) Sections of WT (*n* = 4) and *vegfaa*$^{-/-}$ (*n* = 4) ventricles at 45 dpi stained with AFOG to identify scar (blue), fibrin (red), and muscle (orange). (*H*) Microarray profiling of *vegfaa*$^{+/+}$ and *vegfaa*$^{-/-}$ ventricles. Data are shown relative to *vegfaa*$^{+/+}$ ventricles, which are set at 1 (dashed line). (Scale bars: *B–E*, 50 μm; *F* and *G*, 100 μm.)

To test the requirements for *vegfaa* in revascularization after cardiac injury, *vegfaa* mutants were cryoinjured, and damaged ventricles were analyzed at 40 hpi, a time when revascularization in control fish is well underway and the vascular plexus has formed (Fig. 1*C*). Interestingly, at 40 hpi, *vegfaa* mutants exhibited delayed revascularization and a disorganized plexus (Fig. 2 *B* and *C*). Despite these defects, *vegfaa* mutants were able to further revascularize the injured area, and by 4 dpi, the disorganized plexus had further expanded, populating the damaged ventricle (Fig. 2 *D* and *E*). At 45 dpi, *vegfaa* mutants did not show obvious scar tissue and new muscle was observed in the injured area (Fig. 2 *F* and *G* and Fig. S5 *G* and *H*), which was covered by coronary vessels (Fig. S5 *I–K*).

To investigate the possible mechanisms *vegfaa* mutants use to compensate for the lack of *vegfaa*, we performed transcriptomic profiling of *vegfaa*$^{+/+}$ and *vegfaa*$^{-/-}$ ventricles. We found that other members of the *vegf* family such as *vegfab* and *vegfc*, and genes encoding molecules known to increase VEGF availability and activity, such us *plasminogen* (*plg*) and *collagen and calcium binding EGF domains 1* (*ccbe1*), were up-regulated in *vegfaa* mutants (Fig. 2*H*). These findings are in line with previous observations that *vegfaa*$^{-/-}$ embryos express higher levels of *vegfab* mRNA (28). Moreover, we found that glycolytic genes and hypoxia responsive genes were up-regulated in *vegfaa* mutant hearts (Fig. S5 *L* and *M*), suggesting that as a consequence of the deficient coronary network in *vegfaa*$^{-/-}$ hearts, oxygenation was reduced and nonoxidative metabolism was stimulated. These data, together with the reduced heart rate, suggest that *vegfaa*$^{-/-}$ hearts might experience myocardial hibernation, as described for hypoperfused hearts generated by cardiac suppression of Vegf signaling (30). Overall, these results indicate that rescued *vegfaa* mutants trigger potentially compensating mechanisms that allow the development of a coronary network.

Induction of *dn-vegfaa* Expression Blocks Revascularization of the Damaged Area. Next, we set out to develop a tool that would allow us to efficiently block revascularization following injury. We generated an inducible transgenic line expressing a dn-Vegfaa isoform under the control of the zebrafish *heatshock 70-like* (*hsp70l*) promoter. To visualize the effects of dn-Vegfaa overexpression in the vasculature, *Tg(hsp70l:dn-vegfaa)* fish were crossed into the endothelial-specific *Tg(etv2:EGFP)* line. *Tg(hsp70l:dn-vegfaa);Tg(etv2:EGFP)* embryos heatshocked every 12 h from tailbud stage until 48 hpf show severe defects in angiogenesis and primary sprouting is blocked whereas their WT clutchmates appeared unaffected (Fig. S6 *A* and *B*). To test whether *Tg(hsp70l:dn-vegfaa)* fish up-regulate the same genes as *vegfaa* mutants, we heatshocked WT and *Tg(hsp70l:dn-vegfaa)* adults for 4 d and analyzed by qPCR the expression of *vegfab*, *plg*, *vegfc*, and *ccbe1*. Our results show that induction of dn-Vegfaa did not trigger the up-regulation of these genes (Fig. S6*C*).

Next, to analyze whether the stress caused by cryoinjury induces *hsp70l* expression, we injured transgenic animals expressing a membrane marker fused to GFP, *Tg(hsp70l:GFP-podxl)* (31). At 1 and 2 dpi, we observed an overall increase in GFP signal (Fig. S7 *A–E*). Moreover, we analyzed *hsp70l* mRNA levels by qPCR at 6 hpi and 1, 2, 3, and 5 dpi, observing that *hsp70l* expression significantly increased from 6 hpi to 2 dpi and dropping to basal levels by 3 dpi (Fig. S7*F*).

VEGFA can be bound to the cell surface or in the extracellular matrix (ECM) (32) and, thus, it might be unbound after injury. Therefore, to minimize the effect of this Vegfa pool, we heatshocked *Tg(hsp70l:dn-vegfaa)* and WT clutchmates the day before cryoinjury. Subsequently, animals received daily heatshocks, starting at 24 hpi. At 40 hpi, induction of the *dn-vegfaa* transgene had efficiently blocked revascularization. In contrast to WT hearts, which exhibited a well-developed vascular plexus and large vessels invading the injured area at 40 hpi (Fig. 3*B*), the vast majority of *etv2:*EGFP^{+} cells in the injured area at 40 hpi corresponded to

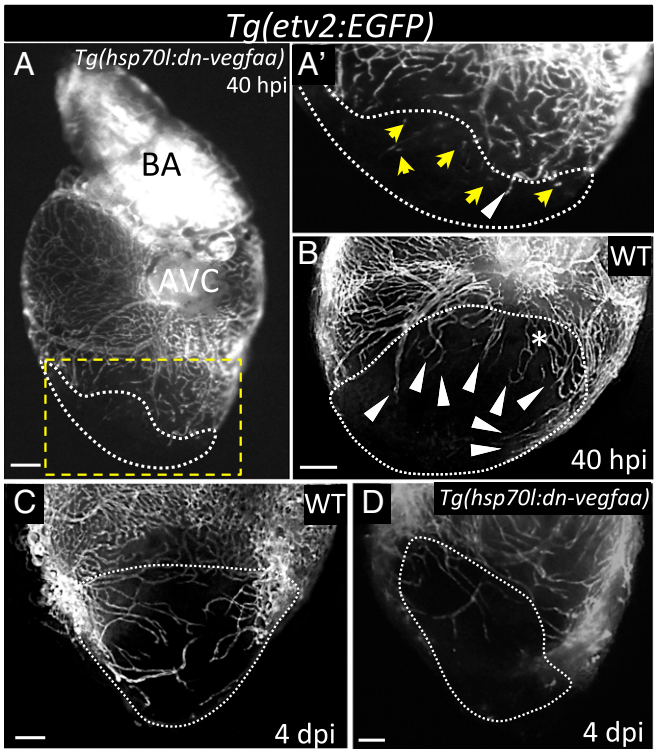

Fig. 3. Induction of *dn-vegfaa* expression blocks revascularization of the damaged area. (*A*) *Tg(hsp70l:dn-vegfaa);Tg(etv2:EGFP)* ventricle at 40 hpi ($n = 5$). (*A′*) *Inset* shows high-magnification image of the injured area. (*B*) *Tg(etv2:EGFP)* WT ventricle at 40 hpi ($n = 5$). (*C*) *Tg(etv2:EGFP)* WT ventricle at 4 dpi ($n = 5$). (*D*) *Tg(hsp70l:dn-vegfaa);Tg(etv2:EGFP)* heart at 4 dpi ($n = 3$). White arrowheads point to coronary vessels sprouting into the injured area; yellow arrows point to disconnected endothelial cells; asterisk mark an area of coronary plexus. Dotted lines delineate the injured area. AVC, atrioventricular canal; BA, bulbus arteriosus. (Scale bar: 100 μm.)

disconnected vessels (Fig. 3 *A* and *A′*). Moreover, vascular invasion remained inhibited at 4 dpi after daily heatshock (Fig. 3 *C* and *D*).

Next, to test whether the dn-Vegfaa isoform might affect Vegfc signaling, we heatshocked *Tg(hsp70l:dn-vegfaa)* and WT clutchmates at 30 hpf, before the onset of secondary sprouting, a well-documented *vegfc*-dependent process (33). Embryos received a 1-h heatshock every 12 h until 5 dpf. At 5 dpf, both WT and *Tg(hsp70l:dn-vegfaa)* larvae had a lymphatic thoracic duct (Fig. S8 *A* and *B*), which is missing in *vegfc*, *vegfr3*, and *ccbe1* mutants (34–36). Thus, our results suggest that overexpression of dn-Vegfaa does not effectively interfere with Vegfc signaling. Together, these data indicate that inducing the expression of *dn-vegfaa* prevents revascularization of the injured area.

Revascularization of the Damaged Area Supports CM Proliferation. To test the impact that blockade of revascularization might have during heart regeneration, we heatshocked *Tg(hsp70l:dn-vegfaa)* and WT clutchmates until 7 dpi, a stage of peak CM proliferation. We noted that by 7 dpi, WT hearts showed a dense endothelial network covering the surface (Fig. 4*A*) and the inside of the injured area (Fig. 4*B*). In contrast, *Tg(hsp70l:dn-vegfaa)* hearts failed to revascularize, displaying only a few superficial vessels in the damaged area and exhibiting a nearly 75% reduction in vascular density compared with WT ventricles (Fig. 4 *C–E*). Next, we tested whether blocking vascular invasion affected CM proliferation. Following the same heatshock regimen that prevented revascularization, we assessed WT and *Tg(hsp70l:dn-vegfaa)* ventricles at 7 dpi. We observed a 60% reduction in CM proliferation in *Tg(hsp70l:dn-vegfaa)* (6.48%) compared with WT (16.32%) (Fig. 4 *F–H*). Because previous studies have reported that inhibition of Vegfa function can affect CM contractility (37), we heatshocked uninjured WT and *Tg(hsp70l:dn-vegfaa)* adults for 7 d and analyzed their heart rate by ultrasound. Our results indicate that overexpression of dn-Vegfaa on its own did not significantly alter heart rate (Fig. S9*A*). In addition, we examined the effect of dn-Vegfaa on CM apoptosis. TUNEL staining of ventricles from *Tg(hsp70l:dn-vegfaa)* and WT siblings heatshocked until 7 dpi revealed no differences in CM apoptosis (Fig. S9 *B* and *C*). Altogether, these results show that revascularization enables heart regeneration, at least in part, by supporting CM proliferation.

Blockade of Early Revascularization Prevents Vascular Invasion and Heart Regeneration. We next set out to determine whether revascularization is restricted in time or whether the zebrafish

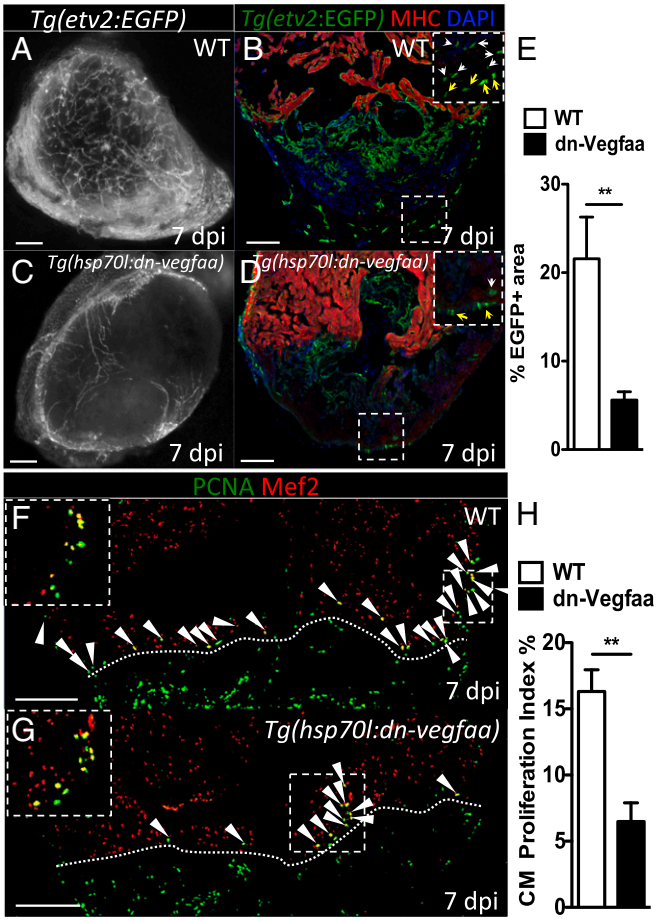

Fig. 4. Revascularization of the damaged area supports CM proliferation. (*A* and *C*) Images of the apex of *Tg(etv2:EGFP)* WT and *Tg(hsp70l:dn-vegfaa);Tg(etv2:EGFP)* ventricles at 7 dpi. WT and *Tg(hsp70l:dn-vegfaa)* were daily heatshocked. (*B* and *D*) Sections of *Tg(etv2:EGFP)* WT and *Tg(hsp70l:dn-vegfaa);Tg(etv2:EGFP)* ventricles. CMs are immunostained with anti-MHC antibody (red), and nuclei counterstained with DAPI (blue). *Insets* show high-magnification images of the coronaries on the surface of the heart (yellow arrows) and in the damaged area (white arrows). (*E*) Quantification of coronary vessel formation in the injured area. The percentage of *etv2*:EGFP$^+$ area was measured relative to total injured area in WT ventricles ($n = 6$) and *Tg(hsp70l:dn-vegfaa)* ventricles ($n = 5$). (*F* and *G*) Sections from *Tg(etv2:EGFP)* WT and *Tg(hsp70l:dn-vegfaa);Tg(etv2:EGFP)* ventricles stained with anti-Mef2 (red) and anti-PCNA (green) antibodies. Arrowheads point to Mef2$^+$/PCNA$^+$ nuclei. *Insets* show high-magnification images of Mef2$^+$/PCNA$^+$ nuclei. (*H*) Quantification of CM proliferation in WT ($n = 5$) and *Tg(hsp70l:dn-vegfaa)* ($n = 5$) ventricles at 7 dpi. Data are expressed as mean ± SEM, $^{**}P < 0.001$. Dotted lines delineate the injured area. (Scale bars: 100 μm.)

heart retains vascular plasticity during the whole regenerative process. To address this question, we heatshocked WT and *Tg(hsp70l:dn-vegfaa)* zebrafish until 4 dpi, coinciding with the onset of CM proliferation, and assessed ventricles at 21, 45, 75, and 150 dpi. We noted that at 21 dpi, in a significant number of *Tg(hsp70l:dn-vegfaa)* ventricles ($3 < 5$), some tissue appeared to be missing in the damaged area compared with WT ventricles where partial replenishment with healthy tissue was already observed (Fig. 5 *A*–*B′*). Whereas WT ventricles showed an extensive coronary network in the damaged area, *Tg(hsp70l:dn-vegfaa)* ventricles displayed a significantly reduced number of vessels that failed to form a mature network. To assess the impact this dramatic reduction in revascularization had on tissue scarring, we followed the same heatshock regimen and stained sectioned ventricles from WT and *Tg(hsp70l:dn-vegfaa)* fish with anti-MHC antibodies to visualize CMs, or acid fuchsin orange G (AFOG) to visualize collagen, fibrin, and CMs. At 21 dpi, no obvious differences in muscle replenishment were observed (Fig. 5 *C* and *D*). Assessment of scar composition showed that in 21 dpi WT ventricles, a large portion of fibrin had been replaced by collagen (Fig. 5*E*). In contrast, in *Tg(hsp70l:dn-vegfaa)* ventricles, the injured zone was filled almost exclusively by collagen (Fig. 5*F*). These results indicate that in the absence of revascularization, the scarring process was altered, because the fibrin portion of the injured area was lost and instead a fibrotic scar was prominent.

Next, we followed the same heatshock regimen and ventricles were analyzed at 45 dpi. By 45 dpi, WT animals exhibited a fully recovered coronary network and new muscle replaced the scar (Fig. 5 *G*, *I*, and *K*). Strikingly, *Tg(hsp70l:dn-vegfaa)* ventricles failed to regenerate, displaying only a few vessels in the damaged area (Fig. 5*H*). Moreover, *Tg(hsp70l:dn-vegfaa)* ventricles were unable to replace the damaged myocardium with new CMs and retained a fibrotic scar composed primarily of collagen (Fig. 5 *J* and *L*). To assess whether interruption of fast revascularization blocked, rather than simply delayed, heart regeneration, we followed the same heatshock regimen and analyzed ventricles at 75 and 150 dpi. As observed at 45 dpi, *Tg(hsp70l:dn-vegfaa)* ventricles at 75 and 150 dpi failed to revascularize the injured area and exhibited large collagen scars (Fig. 5 *M*–*P*). Importantly, at both these stages, all *Tg(hsp70l:dn-vegfaa)* ventricles lacked a portion of the initially damaged tissue (Fig. 5*O*). Overall, these data show that blocking early revascularization abrogates the regenerative capacity of the zebrafish heart.

Discussion

The failure of clinical trials in therapeutic neovascularization revealed the urgent need to better understand the biology behind angiogenic revascularization (18, 38). Here, we show that zebrafish mount a strong angiogenic revascularization response remarkably early after injury. Moreover, we developed an inducible transgenic line, expressing *dn-vegfaa*, that exerts an antiangiogenic effect, allowing one to efficiently prevent vascular invasion of the damaged area. Using this in vivo tool, we show how blocking early vascular sprouting is sufficient to abrogate heart regeneration. Our results indicate that early angiogenic revascularization provides a vascular framework essential to support replenishment of the damaged area with healthy tissue.

Previous studies in zebrafish proposed neovascularization as a late event based on the observation that the first vessels could be seen in the injured area at 7 dpi (12, 16). These studies used resection, whereby the damaged region is removed, preventing any possibility to visualize neovascularization of the injured area. Recently, using cryoinjury, Gonzalez-Rosa et al. observed new vessels in the injured zone at 3 dpi (5). Our results show that new vessels can be observed in the injured area as early as 15 hpi, challenging the established model of neovascularization as a late event. It has been suggested that regenerated coronary vessels derive mainly from preexisting endothelial cells (17). Supporting this notion, we observed that neovascularization was happening mainly by angiogenic sprouting from preexisting vessels. However, based on previous results and ours, we cannot completely exclude the possibility that a small percentage of the newly formed vessels have a nonangiogenic origin.

A number of growth factors are known to regulate angiogenesis. Namely, VEGFA has received most of the attention because of its pleiotropic effects and potency in promoting proliferation and differentiation of the various cell lineages involved in the formation of new vessels during development and in pathological states. However, disappointing results from a number of clinical trials reveal the need to optimize the mode, dosage, and time of delivery of VEGFA (18). In this light, recent studies have shown that fast and brief administration of human VEGFA at the time of myocardial infarction improves neovascularization, heart function, and long-term survival in mice (21). Similarly, we observed that in zebrafish, *vegfaa* expression was up-regulated by 24 hpi, supporting an early role for this growth factor during neovascularization. We did not observe a significant up-regulation of *vegfaa* or *vegfab* before the time of sprouting initiation.

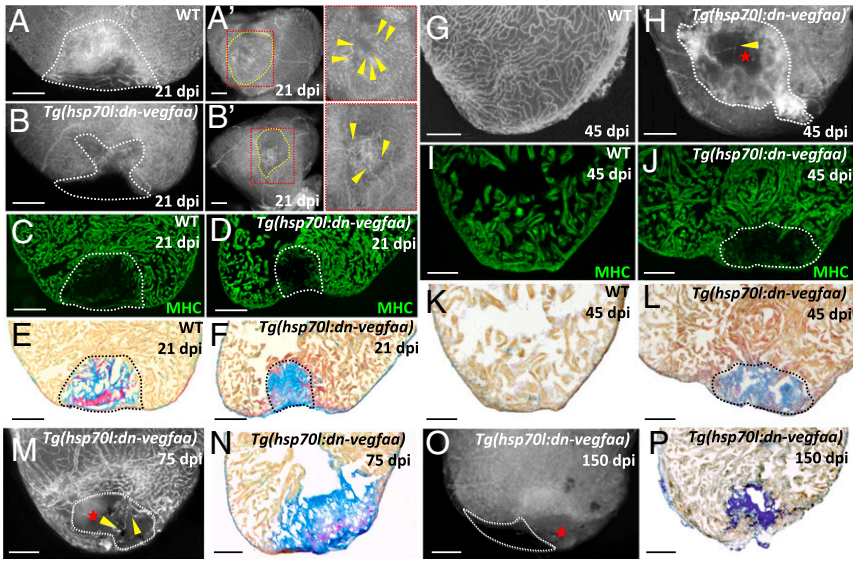

Fig. 5. Blockade of early revascularization prevents vascular invasion and heart regeneration. (*A* and *B*) *Tg(etv2:EGFP)* WT ($n = 5$) and *Tg(hsp70l:dn-vegfaa);Tg(etv2:EGFP)* ($n = 5$) ventricles at 21 dpi. (*A′* and *B′*) View of the apex of *Tg(etv2:EGFP)* WT and *Tg(hsp70l:dn-vegfaa);Tg(etv2:EGFP)* ventricles at 21 dpi. Yellow dotted lines delineate the injured area. *Insets* (red dotted boxes) show high-magnification images of the injured area. Yellow arrowheads point to coronaries in the injured area. (*C* and *D*) Sections of *Tg(etv2:EGFP)* WT ($n = 5$) and *Tg(hsp70l:dn-vegfaa);Tg(etv2:EGFP)* ($n = 5$) ventricles at 21 dpi. CMs are immunostained with anti-MHC antibody (green). (*E* and *F*) Sections of WT ($n = 4$) and *Tg(hsp70l:dn-vegfaa)* ($n = 5$) ventricles at 21 dpi stained with AFOG to identify collagen (blue) and fibrin (red) deposition. (*G* and *H*) *Tg(etv2:EGFP)* WT ($n = 5$) and *Tg(hsp70l:dn-vegfaa);Tg(etv2:EGFP)* ($n = 4$) ventricles at 45 dpi. (*I* and *J*) Sections of *Tg(etv2:EGFP)* WT ($n = 5$) and *Tg(hsp70l:dn-vegfaa);Tg(etv2:EGFP)* ($n = 4$) ventricles at 45 dpi. CMs are immunostained with anti-MHC antibody (green). (*K* and *L*) Sections of WT ($n = 4$) and *Tg(hsp70l:dn-vegfaa)* ($n = 4$) ventricles at 45 dpi stained with AFOG to identify scar (blue) and fibrin (red) deposition. (*M* and *O*) *Tg(hsp70l:dn-vegfaa);Tg(etv2:EGFP)* ventricles at 75 ($n = 4$) and 150 ($n = 4$) dpi. (*N* and *P*) Sections of *Tg(hsp70l:dn-vegfaa)* ventricles at 75 ($n = 4$) and 150 ($n = 4$) dpi stained with AFOG. Dotted lines delineate the injured area. Red stars mark nonvascularized areas. (Scale bars: 100 μm.)

CELL BIOLOGY

This result may indicate that ECM-bound Vegf might be readily available after injury upon ECM degradation or remodeling (32).

Using a recently developed *vegfaa* mutant (28), we found that rescued *vegfaa*$^{-/-}$ adult fish displayed coronary vessels. It has been recently shown that the formation of zebrafish coronaries starts at 1–2 mo of age (27), indicating that *vegfaa* mutants might develop compensatory mechanisms to form a coronary network, as suggested by Rossi et al. (28). To completely block angiogenic revascularization after injury, we developed an inducible *dn-vegfaa* line. We showed that blockade of early angiogenic sprouting impacts CM proliferation and arrests the capacity of the zebrafish heart to regenerate. Considering when sprouting starts after injury, it is tempting to hypothesize that newly formed coronaries are the first tissue to invade the damaged area in zebrafish. Therefore, impairing early angiogenic revascularization prevents timely invasion of the damaged tissue, which might impact the subsequent steps of the regenerative program.

Taken together, our results show that the injured zebrafish heart is able to mount a fast angiogenic revascularization to support heart regeneration. Here, we devised an inducible in vivo reagent that specifically blocks vessel sprouting during development and in pathological states. Using this tool, we showed that blockade of early postinjury sprouting cannot be overcome at later stages, highlighting the importance of timely revascularization. Thus, our results pave the way for future studies using the zebrafish model to understand the fast angiogenic revascularization process after injury. These studies should facilitate the tailoring of more efficient therapies aiming to bridge preclinical and clinical phase studies in therapeutic angiogenesis.

Materials and Methods

Detailed materials and methods are available in *SI Materials and Methods*.

Zebrafish. Procedures involving animals were approved by the veterinary department of the Regional Board of Darmstadt.

Heart Explant Cultures. Heart explant culture were performed as previously described (25).

Echocardiography. Echocardiographic measurements adult hearts were performed as previously described (39).

Coronary Vessel Quantification. Coronary vessel formation in the injured area was quantified as previously described (16).

ACKNOWLEDGMENTS. We thank Ken Poss, Michel Bagnat, and Arndt Siekmann for lines; Maria Missinato for sharing protocols; and Nana Fukuda, the Max Planck Institute Fluorescence-activated cell sorting service group, and Beate Grohmann for assistance. This work was supported by California Institute for Regenerative Medicine Grant TG2-01153 (to S.C.M.) and the Max Planck Society (D.Y.R.S.).

1. Cowie MR, et al. (2014) Improving care for patients with acute heart failure: Before, during and after hospitalization. *ESC Heart Failure* 1(2):110–145.
2. Bergmann O, et al. (2009) Evidence for cardiomyocyte renewal in humans. *Science* 324(5923):98–102.
3. Senyo SE, et al. (2013) Mammalian heart renewal by pre-existing cardiomyocytes. *Nature* 493(7432):433–436.
4. Poss KD, Wilson LG, Keating MT (2002) Heart regeneration in zebrafish. *Science* 298(5601):2188–2190.
5. González-Rosa JM, Martín V, Peralta M, Torres M, Mercader N (2011) Extensive scar formation and regression during heart regeneration after cryoinjury in zebrafish. *Development* 138(9):1663–1674.
6. Schnabel K, Wu CC, Kurth T, Weidinger G (2011) Regeneration of cryoinjury induced necrotic heart lesions in zebrafish is associated with epicardial activation and cardiomyocyte proliferation. *PLoS One* 6(4):e18503.
7. Chablais F, Veit J, Rainer G, Jaźwińska A (2011) The zebrafish heart regenerates after cryoinjury-induced myocardial infarction. *BMC Dev Biol* 11:21.
8. Wang J, et al. (2011) The regenerative capacity of zebrafish reverses cardiac failure caused by genetic cardiomyocyte depletion. *Development* 138(16):3421–3430.
9. Kikuchi K, et al. (2010) Primary contribution to zebrafish heart regeneration by gata4(+) cardiomyocytes. *Nature* 464(7288):601–605.
10. Jopling C, et al. (2010) Zebrafish heart regeneration occurs by cardiomyocyte dedifferentiation and proliferation. *Nature* 464(7288):606–609.
11. Kikuchi K, et al. (2011) Retinoic acid production by endocardium and epicardium is an injury response essential for zebrafish heart regeneration. *Dev Cell* 20(3):397–404.
12. Lepilina A, et al. (2006) A dynamic epicardial injury response supports progenitor cell activity during zebrafish heart regeneration. *Cell* 127(3):607–619.
13. González-Rosa JM, Peralta M, Mercader N (2012) Pan-epicardial lineage tracing reveals that epicardium derived cells give rise to myofibroblasts and perivascular cells during zebrafish heart regeneration. *Dev Biol* 370(2):173–186.
14. Kikuchi K, et al. (2011) tcf21+ epicardial cells adopt non-myocardial fates during zebrafish heart development and regeneration. *Development* 138(14):2895–2902.
15. Zhou B, et al. (2011) Adult mouse epicardium modulates myocardial injury by secreting paracrine factors. *J Clin Invest* 121(5):1894–1904.
16. Kim J, et al. (2010) PDGF signaling is required for epicardial function and blood vessel formation in regenerating zebrafish hearts. *Proc Natl Acad Sci USA* 107(40):17206–17210.
17. Zhao L, et al. (2014) Notch signaling regulates cardiomyocyte proliferation during zebrafish heart regeneration. *Proc Natl Acad Sci USA* 111(4):1403–1408.
18. Taimeh Z, Loughran J, Birks EJ, Bolli R (2013) Vascular endothelial growth factor in heart failure. *Nat Rev Cardiol* 10(9):519–530.
19. Hudlicka O, Brown M, Egginton S (1992) Angiogenesis in skeletal and cardiac muscle. *Physiol Rev* 72(2):369–417.
20. Carmeliet P, et al. (1999) Impaired myocardial angiogenesis and ischemic cardiomyopathy in mice lacking the vascular endothelial growth factor isoforms VEGF164 and VEGF188. *Nat Med* 5(5):495–502.
21. Zangi L, et al. (2013) Modified mRNA directs the fate of heart progenitor cells and induces vascular regeneration after myocardial infarction. *Nat Biotechnol* 31(10):898–907.
22. Bussmann J, et al. (2010) Arteries provide essential guidance cues for lymphatic endothelial cells in the zebrafish trunk. *Development* 137(16):2653–2657.
23. Wang Y, et al. (2010) Moesin1 and Ve-cadherin are required in endothelial cells during in vivo tubulogenesis. *Development* 137(18):3119–3128.
24. Xu C, et al. (2014) Arteries are formed by vein-derived endothelial tip cells. *Nat Commun* 5:5758.
25. Wang J, Cao J, Dickson AL, Poss KD (2015) Epicardial regeneration is guided by cardiac outflow tract and Hedgehog signalling. *Nature* 522(7555):226–230.
26. Sacilotto N, et al. (2013) Analysis of Dll4 regulation reveals a combinatorial role for Sox and Notch in arterial development. *Proc Natl Acad Sci USA* 110(29):11893–11898.
27. Harrison MRM, et al. (2015) Chemokine-guided angiogenesis directs coronary vasculature formation in zebrafish. *Dev Cell* 33(4):442–454.
28. Rossi A, et al. (2015) Genetic compensation induced by deleterious mutations but not gene knockdowns. *Nature* 524(7564):230–233.
29. Rossi A, et al. (2016) Regulation of Vegf signaling by natural and synthetic ligands. *Blood*, 10.1182/blood-2016-04-711192.
30. May D, et al. (2008) Transgenic system for conditional induction and rescue of chronic myocardial hibernation provides insights into genomic programs of hibernation. *Proc Natl Acad Sci USA* 105(1):282–287.
31. Navis A, Marjoram L, Bagnat M (2013) Cftr controls lumen expansion and function of Kupffer's vesicle in zebrafish. *Development* 140(8):1703–1712.
32. Ferrara N (2010) Binding to the extracellular matrix and proteolytic processing: Two key mechanisms regulating vascular endothelial growth factor action. *Mol Biol Cell* 21(5):687–690.
33. Hogan BM, et al. (2009) Ccbe1 is required for embryonic lymphangiogenesis and venous sprouting. *Nat Genet* 41(4):396–398.
34. Hogan BM, et al. (2009) Vegfc/Flt4 signalling is suppressed by Dll4 in developing zebrafish intersegmental arteries. *Development* 136(23):4001–4009.
35. Le Guen L, et al. (2014) Ccbe1 regulates Vegfc-mediated induction of Vegfr3 signaling during embryonic lymphangiogenesis. *Development* 141(6):1239–1249.
36. Villefranc JA, et al. (2013) A truncation allele in vascular endothelial growth factor c reveals distinct modes of signaling during lymphatic and vascular development. *Development* 140(7):1497–1506.
37. Rottbauer W, et al. (2005) VEGF-PLCgamma1 pathway controls cardiac contractility in the embryonic heart. *Genes Dev* 19(13):1624–1634.
38. Molin D, Post MJ (2007) Therapeutic angiogenesis in the heart: Protect and serve. *Curr Opin Pharmacol* 7(2):158–163.
39. González-Rosa JM, et al. (2014) Use of echocardiography reveals reestablishment of ventricular pumping efficiency and partial ventricular wall motion recovery upon ventricular cryoinjury in the zebrafish. *PLoS One* 9(12):e115604.
40. Lawson ND, Weinstein BM (2002) In vivo imaging of embryonic vascular development using transgenic zebrafish. *Dev Biol* 248(2):307–318.
41. Jin SW, Beis D, Mitchell T, Chen JN, Stainier DYR (2005) Cellular and molecular analyses of vascular tube and lumen formation in zebrafish. *Development* 132(23):5199–5209.
42. Proulx K, Lu A, Sumanas S (2010) Cranial vasculature in zebrafish forms by angioblast cluster-derived angiogenesis. *Dev Biol* 348(1):34–46.
43. Roman BL, et al. (2002) Disruption of acvrl1 increases endothelial cell number in zebrafish cranial vessels. *Development* 129(12):3009–3019.
44. Huang CJ, Tu CT, Hsiao CD, Hsieh FJ, Tsai HJ (2003) Germ-line transmission of a myocardium-specific GFP transgene reveals critical regulatory elements in the cardiac myosin light chain 2 promoter of zebrafish. *Dev Dyn* 228(1):30–40.
45. Muller YA, et al. (1997) Vascular endothelial growth factor: Crystal structure and functional mapping of the kinase domain receptor binding site. *Proc Natl Acad Sci USA* 94(14):7192–7197.
46. Detrich HW, 3rd, et al. (1995) Intraembryonic hematopoietic cell migration during vertebrate development. *Proc Natl Acad Sci USA* 92(23):10713–10717.
47. Sander V, Suñe G, Jopling C, Morera C, Izpisua Belmonte JC (2013) Isolation and in vitro culture of primary cardiomyocytes from adult zebrafish hearts. *Nat Protoc* 8(4):800–809.